A GCM Parameterization for the Shortwave Radiative Properties of Water Clouds

A. SLINGO

National Center for Atmospheric Research, Boulder, Colorado*

1 August 1988 and 21 November 1988

ABSTRACT

A new parameterization is presented for the shortwave radiative properties of water clouds, which is fast enough to be included in general circulation models (GCMs). It employs the simple relationships found by Slingo and Schrecker for the optical depth, single scatter albedo and asymmetry parameter of cloud drops as functions of the cloud liquid water path and equivalent radius of the drop size distribution. The cloud radiative properties are then obtained from standard two-stream equations for a homogeneous layer. The effect of water vapor absorption within the cloud is ignored in this version, leading to a small underestimate of the cloud absorption. The parameterization is compared with other schemes and with aircraft observations. It performs satisfactorily even when only four spectral bands are employed. The explicit separation of the dependence of the derived cloud radiative properties on the liquid water path and equivalent radius is new, and should prove valuable for climate change investigations.

1. Introduction

Clouds exert a profound influence on the earth's radiation budget, and thus on the radiative driving of the climate system. Climate models therefore need to incorporate parameterizations for the radiative effects of clouds which are as accurate as possible. In studies of the role of clouds in climate change, the cloud radiative properties have generally been assumed to be constant, either by the use of constant optical depths or through the specification of fixed bulk properties such as the transmissivity and reflectivity (Wetherald and Manabe 1988). The effects of clouds in such studies have thus been restricted to those associated with changes in cloud amounts, although these can be extremely important, producing positive feedbacks which amplify the response to the applied perturbation (Schlesinger and Mitchell 1987).

It is unlikely that cloud radiative properties will remain constant during climate change. These properties are strong functions of the liquid water path and drop size distribution (for water clouds) and mechanisms whereby each of these parameters may change have been proposed. First, a warmer atmosphere can hold more water vapor, which is presumed to lead to higher cloud liquid water contents and hence to more reflective clouds (Paltridge 1980). Recent estimates of the magnitude of this negative feedback suggest that it may be comparable with that due to changes in cloud cover (Somerville and Remer 1984; Roeckner et al. 1987). Second, pollution can also increase cloud reflectivities, by providing additional cloud condensation nuclei (CCN) which nucleate more, but smaller, drops for a given liquid water path and hence increase the cloud optical depth. Twomey et al. (1984) suggested that the cooling effect of such changes may be comparable with the heating produced by increased concentrations of atmospheric carbon dioxide. Evidence that pollution can influence cloud radiative properties was presented by Coakley et al. (1987). A further mechanism was proposed by Charlson et al. (1987), who argued that dimethylsulfide released into the atmospheric boundary layer by marine phytoplankton serves as the dominant source of CCN in remote regions, so that changes in the plankton population may also alter the cloud reflectivities and hence climate.

Since the mechanisms mentioned above act independently of one another, future changes in cloud liquid water contents and drop size distributions are also likely to be independent. In addition, further modeling studies of each mechanism are required. This suggests the need for a parameterization which separates the dependence of the cloud radiative properties on these two parameters. This provided the motivation for the parameterization described below. Previous studies in this area (Liou and Wittman 1979; Stephens et al. 1984) do not provide such a separation, a restriction which may limit their value in climate change investigations.

* The National Center for Atmospheric Research is sponsored by the National Science Foundation.

Corresponding author address: A. Slingo, NCAR, P.O. Box 3000, Boulder, CO 80307-3000.

© 1989 American Meteorological Society

2. Description of parameterization

Slingo and Schrecker (1982, hereafter SS) developed a 24-band shortwave radiation scheme based on the vertically inhomogeneous Delta–Eddington code of Wiscombe (1977). They showed that, for a given spectral interval i, the single scattering properties of typical water clouds could be parameterized in terms of the liquid water path (LWP) and equivalent radius of the drop size distribution (r_e)

$$\tau_i = \mathrm{LWP}\left(a_i + \frac{b_i}{r_e}\right) \tag{1}$$

$$1 - \tilde{\omega}_i = c_i + d_i \cdot r_e \tag{2}$$

$$g_i = e_i + f_i \cdot r_e, \tag{3}$$

where τ_i is the cloud optical depth, $\tilde{\omega}_i$ is the single scatter albedo and g_i is the asymmetry parameter. These relationships were derived for values of r_e from 4.2 to 16.6 μm and are not necessarily valid outside this range. LWP (g m^{-2}) and r_e (μm) are defined as follows

$$\mathrm{LWP} = \int_{\text{cloud base}}^{\text{cloud top}} \mathrm{LWC}\, dz \tag{4}$$

$$r_e = \int_0^\infty n(r) r^3 dr \Big/ \int_0^\infty n(r) r^2 dr, \tag{5}$$

where LWC is the liquid water content (g m^{-3}) at height z (m), r is the drop radius (μm) and $n(r)$ is the drop size distribution function.

Table 1 lists the values of the coefficients in (1) to (3) and of the fraction w_i of the solar irradiance at the top of the atmosphere in each spectral band. The values of w_i were derived from the data of Thekaekara and Drummond (1971). The approximate wavelength limits of each band are also given in the Table. The exact limits in wavenumbers are listed by SS in their Table 1. Slingo and Schrecker used the full 24-band spectral resolution in their study, but it will be shown that these data can be averaged to as few as four broad bands by a careful choice of the band limits.

Some general circulation models (GCMs) employ radiation schemes based on two-stream multiple scattering codes (Stephens 1984). To implement the parameterization in such models it should therefore be possible to use (1) to (3) directly. However, most GCMs require the bulk cloud radiative properties (i.e., the transmissivity, reflectivity and absorptivity), which

TABLE 1. Values of coefficients* in Eqs. 1–3.

Band i	Spectral limits (μm)	a_i (10^{-2} m^2 g^{-1})	b_i (μm m^2 g^{-1})	c_i	d_i (μm^{-1})	e_i	f_i (10^{-3} μm^{-1})	w_i ($\times 10^6$)
1	0.25–0.30	3.094	1.252	7.90E-7	3.69E-7	0.844	1.558	10 094
2	0.30–0.33	2.944	1.270	−6.50E-7	4.33E-7	0.841	1.680	17 224
3	0.33–0.36	3.308	1.246	−3.00E-7	2.36E-7	0.839	1.946	24 017
4	0.36–0.40	2.801	1.293	1.00E-6	0	0.836	2.153	34 645
5	0.40–0.44	2.668	1.307	0	0	0.840	1.881	50 524
6	0.44–0.48	2.698	1.315	1.00E-6	0	0.820	3.004	59 520
7	0.48–0.52	2.672	1.320	0	0	0.828	2.467	57 464
8	0.52–0.57	2.838	1.300	0	0	0.825	2.776	66 188
9	0.57–0.64	2.831	1.317	−1.20E-6	4.00E-7	0.828	2.492	85 882
10	0.64–0.69	2.895	1.315	−1.20E-7	4.40E-7	0.818	2.989	54 202
11	0.69–0.75	3.115	1.244	−2.70E-7	1.40E-6	0.804	3.520	60 863
12	0.75–0.78	2.650	1.349	2.30E-6	1.70E-6	0.809	3.387	25 044
13	0.78–0.87	2.622	1.362	3.30E-6	2.80E-6	0.806	3.355	68 135
14	0.87–1.00	2.497	1.376	9.80E-6	2.10E-5	0.783	5.035	83 962
15	1.00–1.10	2.632	1.365	−4.60E-5	5.00E-5	0.784	4.745	49 082
16	1.10–1.19	2.589	1.385	−2.80E-5	8.00E-5	0.780	4.989	39 072
17	1.19–1.28	2.551	1.401	6.20E-5	2.60E-4	0.773	5.405	29 133
18	1.28–1.53	2.463	1.420	2.40E-4	8.56E-4	0.754	6.555	65 845
19	1.53–1.64	2.237	1.452	1.20E-4	6.67E-4	0.749	6.931	20 611
20	1.64–2.13	1.970	1.501	1.20E-3	2.16E-3	0.740	7.469	50 793
21	2.13–2.38	1.850	1.556	1.90E-4	2.54E-3	0.769	5.171	14 226
22	2.38–2.91	1.579	1.611	1.23E-1	9.35E-3	0.851	2.814	18 681
23	2.91–3.42	1.950	1.540	4.49E-1	1.54E-3	0.831	6.102	9 588
24	3.42–4.00	−1.023	1.933	2.50E-2	1.22E-2	0.726	6.652	5 205
Values for version 10, 6, 5 and 3 (see footnote to Table 2);								
1	0.25–0.69	2.817	1.305	−5.62E-8	1.63E-7	0.829	2.482	459 760
2	0.69–1.19	2.682	1.346	−6.94E-6	2.35E-5	0.794	4.226	326 158
3	1.19–2.38	2.264	1.454	4.64E-4	1.24E-3	0.754	6.560	180 608
4	2.38–4.00	1.281	1.641	2.01E-1	7.56E-3	0.826	4.353	33 474

* For c_i and d_i, the values are abbreviated using Fortran exponential format.

may be derived by a straightforward application of the two-stream equations for a homogeneous layer. For clarity, the subscript i is omitted from the following equations, which are in the correct order for computation and use the Delta–Eddington approximation and the notation of Zdunkowski et al. (1980). The cosine of the solar zenith angle is denoted by μ_0 and f is the fraction of the scattered direct flux which emerges at zenith angles close to that of the incident beam and which may therefore be added back into the accounting for this beam. The U_1 and U_2 are the reciprocals of the effective cosines for the diffuse upward and downward fluxes respectively, β_0 is the fraction of the scattered diffuse radiation which is scattered into the backward hemisphere and $\beta(\mu_0)$ is the same for the direct radiation:

$$\beta_0 = \frac{3}{7}(1-g) \tag{6}$$

$$\beta(\mu_0) = \frac{1}{2} - \frac{3\mu_0 g}{4(1+g)} \tag{7}$$

$$f = g^2 \tag{8}$$

$$U_1 = \frac{7}{4} \tag{9}$$

$$U_2 = \frac{7}{4}\left[1 - \frac{(1-\tilde{\omega})}{7\tilde{\omega}\beta_0}\right] \tag{10}$$

$$\alpha_1 = U_1[1 - \tilde{\omega}(1-\beta_0)] \tag{11}$$

$$\alpha_2 = U_2\tilde{\omega}\beta_0 \tag{12}$$

$$\alpha_3 = (1-f)\tilde{\omega}\beta(\mu_0) \tag{13}$$

$$\alpha_4 = (1-f)\tilde{\omega}[1-\beta(\mu_0)] \tag{14}$$

$$\epsilon = (\alpha_1^2 - \alpha_2^2)^{1/2} \tag{15}$$

$$M = \frac{\alpha_2}{\alpha_1 + \epsilon} \tag{16}$$

$$E = \exp(-\epsilon\tau) \tag{17}$$

$$\gamma_1 = \frac{(1-\tilde{\omega}f)\alpha_3 - \mu_0(\alpha_1\alpha_3 + \alpha_2\alpha_4)}{(1-\tilde{\omega}f)^2 - \epsilon^2\mu_0^2} \tag{18}$$

$$\gamma_2 = \frac{-(1-\tilde{\omega}f)\alpha_4 - \mu_0(\alpha_1\alpha_4 + \alpha_2\alpha_3)}{(1-\tilde{\omega}f)^2 - \epsilon^2\mu_0^2}. \tag{19}$$

The transmissivity for the direct solar beam is

$$T_{DB} = \exp\left[-(1-\tilde{\omega}f)\frac{\tau}{\mu_0}\right], \tag{20}$$

the diffuse reflectivity for diffuse incident radiation is

$$R_{DIF} = \frac{M(1-E^2)}{(1-E^2M^2)}, \tag{21}$$

the diffuse transmissivity for diffuse incident radiation is

$$T_{DIF} = \frac{E(1-M^2)}{(1-E^2M^2)}, \tag{22}$$

the diffuse reflectivity for direct incident radiation is

$$R_{DIR} = -\gamma_2 R_{DIF} - \gamma_1 T_{DB} T_{DIF} + \gamma_1, \tag{23}$$

and

the diffuse transmissivity for direct incident radiation is

$$T_{DIR} = -\gamma_2 T_{DIF} - \gamma_1 T_{DB} R_{DIF} + \gamma_2 T_{DB}. \tag{24}$$

Note that the total transmission to direct incident radiation is the sum of T_{DB} and T_{DIR}. Simpler forms of these equations are available for the case of conservative scattering ($\tilde{\omega} = 1$; see Zdunkowski et al. 1980). However, for the present work the general equations were preferred, as only three of the 24 SS bands have zero values of c_i and d_i in (2), corresponding to conservative scattering (see Table 1).

In this form, the parameterization ignores the effect of water vapor absorption within the cloud, which both SS and Davies et al. (1984) showed to be less important than the absorption by water drops. This leads to a small underestimate of the total cloud absorption in some of the tests presented later. The inclusion of water vapor absorption is discussed in section 5.

3. Comparisons with observations and other parameterizations

The parameterization is compared with the SS scheme and that of Stephens et al. (1984), using aircraft data for midlatitude marine stratocumulus and for arctic clouds. Comparisons with Liou and Wittman (1979) were found to be unreliable, because of difficulty in determining sufficiently accurate values of the equivalent radius from the information they give on the drop size distributions.

The parameterization was incorporated into the radiation subroutine employed in the U.K. Meteorological Office climate model (Slingo and Pearson 1987). This subroutine (Helios) used fixed vertical resolution based on the model's 11 layers, so it was first generalized to cope with arbitrary vertical resolution. It was then expanded to employ up to 24 shortwave spectral bands, with absorption data for water vapor and ozone in each band derived from the exponential sum fits of the SS scheme. The weak CO_2 absorption at around 2.7 μm wavelength was included by multiplying the CO_2 and H_2O transmissivities in the appropriate band. The CO_2 mixing ratio was assumed to be 330 ppmv. Each of the Helios spectral bands corresponds to one or more of the SS bands, the gaseous absorption data and the coefficients for the parameterization being combined automatically within the subroutine with relative weightings given by the factor w_i listed in Table 1. This feature greatly facilitated the investigation of the optimum

number of spectral bands for the GCM. As an example, if band n of Helios is formed from SS bands j to k, the appropriate value of the coefficient a in (1) is

$$a_n = \sum_{i=j}^{k} a_i w_i / \sum_{i=j}^{k} w_i. \tag{25}$$

This averaging is both simple and computationally efficient, as it minimizes the number of passes which are required through the equations of the parameterization. In principle, the weights in (25) should be based on the spectral distribution of the flux incident at the cloud top, rather than of the extraterrestrial irradiance. In practice, this is less important than the requirement for a minimum number of broad bands to represent the gross spectral features of atmospheric transmission.

Clear-sky comparisons were made with Lacis and Hansen (1974) for ozone and Kratz and Cess (1985) for water vapor. The ozone heating rates agree to within a few tenths of 1 K day^{-1} below 40 km. The water vapor heating rates are within ± 0.2 K day^{-1} in the troposphere. The effects of Rayleigh scattering were ignored in this version of Helios.

The parameterization developed by Stephens (1978) and revised by Stephens et al. (1984) was also programmed into Helios, allowing a direct comparison with the new parameterization. When the contour plots shown by Stephens et al. (1984) were reproduced, spurious maxima were obtained. These were removed by smoothing the data for $(1 - \tilde{\omega}_0)$ in their Table 1(a) to give a more realistic dependence on optical depth. As in Stephens' work, two spectral bands were employed with the boundary between them at 0.75 μm (actually at 13 300 cm^{-1}, the boundary between SS bands 11 and 12). The results for Stephens shown in Tables 2–3 are quite sensitive to the position of this boundary. For example, when only 10 SS bands are combined to form the first Helios band (as in most of the runs with the new parameterization), the cloud absorptions increase by about 15 percent.

The SS scheme was also included in the comparisons. It deals with Rayleigh scattering by atmospheric molecules as well as multiple scattering and absorption by cloud drops and the surface, plus molecular absorption by water vapor and ozone. The scheme has been employed in several investigations and in general has given results (including the cloud absorption) which are in agreement with aircraft radiometer observations to within the experimental errors (Slingo et al. 1982; Nicholls 1984; Herman and Curry 1984; Nicholls and Leighton 1986; Hignett 1987; Foot 1988). Herman and Curry measured some cloud absorptions in excess of those predicted by the SS scheme, as also did Foot. Hignett showed evidence that while the broadband albedo agreed with his data, this was due to compensation between an underestimate in the visible part of the spectrum and an overestimate in the near-infrared.

The solar constant was taken to be 1373 W m^{-2} and the observed temperature and humidity profiles were used. The observed vertical structure of the cloud liquid water content and equivalent radius was resolved in the SS scheme. Helios was run with the cloud occupying a single layer, the base and top being the same as in the SS scheme. The values of LWP and r_e required by the new parameterization were chosen so that both the cloud optical depth and liquid water path were the same as in the SS scheme, given the finite difference approximations made in the latter. For this purpose, the cloud optical depth was calculated as

$$\tau = \frac{3}{2} \int_{\text{cloud base}}^{\text{cloud top}} \frac{\text{LWC}}{r_e}\, dz, \tag{26}$$

where both LWC and r_e are functions of the height z. In Helios, the cloud shortwave properties were calculated assuming that only direct radiation was incident on the cloud top, which is a reasonable assumption for the isolated cloud decks in these comparisons.

One of several minor differences between the SS scheme and Helios is that the former implicitly takes account of the enhancement of water vapor absorption within the cloud by droplet scattering (which increases the effective optical path), whereas the latter ignores this effect because the parameterization only takes account of the liquid water. Some evidence is presented later to show that this leads to a small underestimate of the cloud absorption by the parameterization for clouds of low optical depth.

a. Marine stratocumulus

The JASIN experiment conducted over the North Atlantic Ocean provided an excellent case study of a uniform sheet of marine stratocumulus (Slingo et al. 1982). The solar zenith angle was 43.7°, the surface albedo was 0.05 at all wavelengths and the profiles of liquid water content and equivalent radius were taken from profile C (cf. Figs. 8, 9 and 14 of Slingo et al. 1982). Table 2 shows that both the system albedo (the ratio of the upward flux to the downward flux at the cloud top) and cloud absorption (the ratio of the difference in net downward flux across the cloud to the downward flux at the cloud top) are predicted by the SS scheme to within the experimental errors. These definitions of albedo and absorption are used for consistency with the observations and it should be remembered that they include the effects of multiple reflections between the cloud and surface.

Helios was run with a liquid water path of 151.2 g m^{-2} and equivalent radius 10.35 μm. With 24 bands, the system albedo is close to that from SS, although the cloud absorption is slightly smaller (Table 2). As a first step in exploring the viability of a scheme with a reduced number of bands, the first 10 SS bands were combined into one Helios band extending from 0.25 to 0.69 μm. This 15-band Helios gives results which are very close to the 24-band version, the reason being that clouds act as conservative gray-body scatterers in

TABLE 2. Comparison of observed and modeled cloud shortwave radiative properties (Marine stratocumulus; Slingo et al. 1982).

Source	Number of bands	Configuration of bands*	System albedo (%)	Cloud absorption (%)
Observed	—	—	68 ± 2	7 ± 3
Slingo/Schrecker scheme (SS)	24	—	68.3	7.1
Helios	24	1, 1, 1 · · ·	68.8	6.3
Helios	15	10, 1, 1 · · ·	68.8	6.3
Helios	4	10, 7, 3, 4	68.3	6.9
Helios	4	10, 7, 4, 3	68.7	6.5
Helios	4	10, 6, 5, 3	68.4	7.0
Helios	3	10, 7, 7	66.2	9.6
Helios	3	10, 11, 3	66.8	10.4
Helios	2	10, 14	57.0	25.6
Helios	1	24	51.7	36.4
Stephens	2	11, 13	73.7	10.3

* This indicates the number of SS bands included in each Helios band. For example, the 4-band version 10, 6, 5 and 3 combines SS bands 1 to 10, followed by 11 to 16, 17 to 21 and 22 to 24.

the visible region of the spectrum, so that one spectral band is sufficient. A much more drastic reduction to only 4 Helios bands still gives satisfactory results, the version 10, 6, 5 and 3 being particularly close to SS (see the footnote to Table 2 for an explanation of the terminology). Comparison of the three versions with four bands shows that the results are not particularly sensitive to the location of the band limits in the infrared. However, there is a significant degradation when the number of bands is reduced to three and lower, even when the only change is to combine the two bands in the far infrared. The rapid increase in the predicted cloud absorption as the number of bands is reduced below four is consistent with the findings of SS (1982, their Fig. 5). It is caused by the artificial increase in the fraction of the spectrum available for absorption when the strong wavelength dependence of $(1 - \tilde{\omega})$ is improperly resolved. These results suggest that a minimum of four spectral bands is required. The same conclusion was reached by Zdunkowski et al. (1982, p. 231). The last entry in Table 2 shows that both the system albedo and cloud absorption are increased when Stephens' parameterization is included in Helios. In both cases, the values are slightly higher than the observed.

Similar results were obtained for the cloud observed by Foot (1988), except that the observed cloud absorption was about twice that from the SS scheme. One explanation offered by Foot was the possibility of carbonaceous aerosol within the cloud. The effects of such an aerosol could be taken into account by modifying the single scattering data, as was done to include the effects of Rayleigh scattering in the SS scheme.

b. Arctic clouds

Observations of several cloud decks over the Beaufort Sea were presented by Herman and Curry (1984, hereafter HC), who also showed comparisons with the theoretical cloud radiative properties obtained from runs of the SS scheme. For simplicity, multilevel clouds included by HC have been omitted, but this still leaves 7 cases with low liquid water paths, including a thin altostratus with small drops (F6–P1; see Table 3). The SS scheme was run with the appropriate cloud data listed by HC, and as in the previous tests for consistency Helios was run with values of LWP and r_e taken from the SS scheme. Table 3 lists the values used, which are slightly different from those given by HC in their Table 6, presumably because the latter were obtained from the raw data. The surface albedo prescription in the present runs of the SS scheme was also deliberately crude for consistency with Helios, the HC visible surface albedos being employed in the first ten bands and the near-infrared values in the remainder. As a result, the cloud radiative properties from the SS scheme listed in Table 3 are slightly different from those derived by HC from their own runs of the scheme (their Tables 3 and 5).

TABLE 3. Comparison of observed and modeled cloud shortwave radiative properties (Arctic clouds; Herman and Curry 1984)

			System albedo (%)						Cloud absorption (%)					
			Modeled				Observed[c]		Modeled				Observed[b]	
Flight-profile	LWP[a] (g m^{-2})	r_e[a] (μm)	SS	Helios[b]		Stephens	Ep	Si	SS	Helios[c]		Stephens	Ep	Si
F1–P1	11.96	8.38	68.4	69.1	69.1	70.8	55	73	2.8	2.1	2.0	3.9	23	11
F1–P2	32.35	9.28	71.8	72.7	72.8	75.6	79	82	4.7	3.6	3.6	7.1	1	8
F3–P1	55.01	7.94	69.5	70.0	70.0	72.0	59	73	4.4	3.6	3.7	7.5	15	5
F3–P2	47.28	7.94	69.2	69.5	69.5	72.0	63	80	4.4	3.5	3.6	7.0	17	0
F4–P2	23.18	7.62	60.3	60.3	60.3	63.1	49	53	3.1	2.3	2.3	5.3	12	11
F5–P1	124.30	7.26	78.8	79.4	79.1	78.8	74	78	6.1	5.2	5.7	8.3	7	2
F6–P1	14.85	4.33	62.9	63.2	63.2	59.7	59	66	3.5	2.8	2.8	4.7	23	10

[a] Calculated from the SS runs, which use the observed vertical structure, and employed as input for the Helios runs.
[b] From the 24-band scheme, followed by the 4-band scheme 10, 6, 5 and 3.
[c] The abbreviation Ep refers to measurements with Eppley pyranometers and Si to measurements with silicon detectors.

The radiative properties from Helios listed in Table 3 were obtained with the 24-band scheme and the 4-band scheme denoted 10, 6, 5 and 3. Results from the two versions are generally within about ±0.1 of each other. This is closer than for the JASIN case and is related to the lower optical depths of most of these clouds. The exception is F5–P1, which has a higher liquid water path and a sensitivity to the number of spectral bands which is similar to that for the midlatitude cloud.

The system albedos from Helios are within one percent of those from the SS scheme. However, Helios systematically underestimates the cloud absorption, compared with SS. The ratio of the absorptions is inversely related to the cloud optical depth, being largest for F1–P1 and smallest for F5–P1. This is mainly due to the fact that the new parameterization neglects the contribution of water vapor to the cloud absorption. As noted by HC, the relative importance of water vapor absorption compared with cloud droplet absorption increases as the cloud optical depth is reduced. When the SS scheme was run with the water vapor amounts inside the cloud set to zero, the underestimate was reduced from the maximum of 1.1 percent shown in the table to less than 0.5 percent.

The system albedos from Stephens' parameterization are similar to those from SS and the present scheme. However, the cloud absorptions are higher than those from SS in all cases. For the clouds with the higher liquid water paths this is in part due to an overestimate by Stephens' parameterization, compared with his detailed radiation model (see Fig. 1b of Stephens et al. 1984). However, this only explains part of the difference, suggesting that there are genuine disagreements between the Stephens and SS models which may warrant further investigation.

When comparing the theoretical results with the observations, the errors inherent in making such measurements for optically thin and often inhomogeneous clouds must be remembered. The differences between the radiative properties from the two radiometer systems (denoted Ep and Si in Table 3) are also quite large in some cases. With this in mind, the theoretical properties are not inconsistent with the observations. Herman and Curry noted that the observed cloud absorptions were in some cases much larger than those given by the SS scheme, which is supported by the present work. However, for the case described as 'the best for future detailed radiation studies' (F5–P1), there is reasonable agreement between the observations and theory, with no evidence for anomalously high absorption.

4. Further comparisons with Stephens' parameterization

Comparisons between the results shown in the previous section are complicated by the fact that the new scheme takes account of the observed values of the equivalent radius, whereas Stephens' parameterization effectively chooses its own values based on his liquid water path to optical depth relationship [Stephens 1978; his Eq. (10)]. In addition, gaseous absorption above and below the cloud and multiple reflections between the cloud and surface contribute to the cloud radiative properties. A more controlled comparison was therefore made, in which each parameterization was run in isolation for a range of liquid water paths and solar zenith angles, the value of r_e in the appropriate band of the new scheme being forced to be consistent with Stephens (1978) by deriving it from his (10) and (7). The derived radiative properties in each spectral band were weighted together by the factor w_i in Table 1. The results are intended to provide what may be termed the "intrinsic" cloud radiative properties, which are determined only by the cloud microphysics (although for reasons explained below this is strictly not possible with Stephens' scheme). The 4-band version 10, 6, 5 and 3 of the new parameterization and the 2-band version 11 and 13 of Stephens' scheme were included in this comparison.

Figure 1 shows the results of this comparison in the same format as in Fig. 1 of Stephens et al. (1984), except that the maximum liquid water path is 1000 g m^{-2}. The behavior of the cloud radiative properties is similar for both schemes; the reflectivity increases with liquid water path and solar zenith angle, while the absorptivity increases with liquid water path and decreases with solar zenith angle over most of the domain. The maximum difference between the radiative properties from the two schemes is around 6 percent for the reflectivity and 4 percent for the absorptivity. One notable difference is that the zenith angle dependence of both the reflectivity and absorptivity is much more marked with Stephens' parameterization than with the new scheme, especially at large solar zenith angles. This is presumably because Stephens tuned his parameterization to agree with the results from his detailed radiation model, which was run with the clouds inserted in the U.S. Standard Atmosphere, rather than for the clouds in isolation. His parameterization thus implicitly includes the additional zenith angle dependence brought about by sensitivity to the water vapor absorption above the cloud in that particular atmosphere. If the parameterization were included in a GCM, the effect of the water vapor profile on the cloud radiative properties would effectively be included twice, as GCMs already include their own calculations of the depletion of the solar beam by water vapor. The approach followed in the present paper of developing a parameterization for the "intrinsic" cloud radiative properties only, letting the host GCM take care of the rest of the atmospheric absorption, would appear to be both simpler and more accurate.

A further advantage of the present parameterization is the explicit dependence on the equivalent radius of

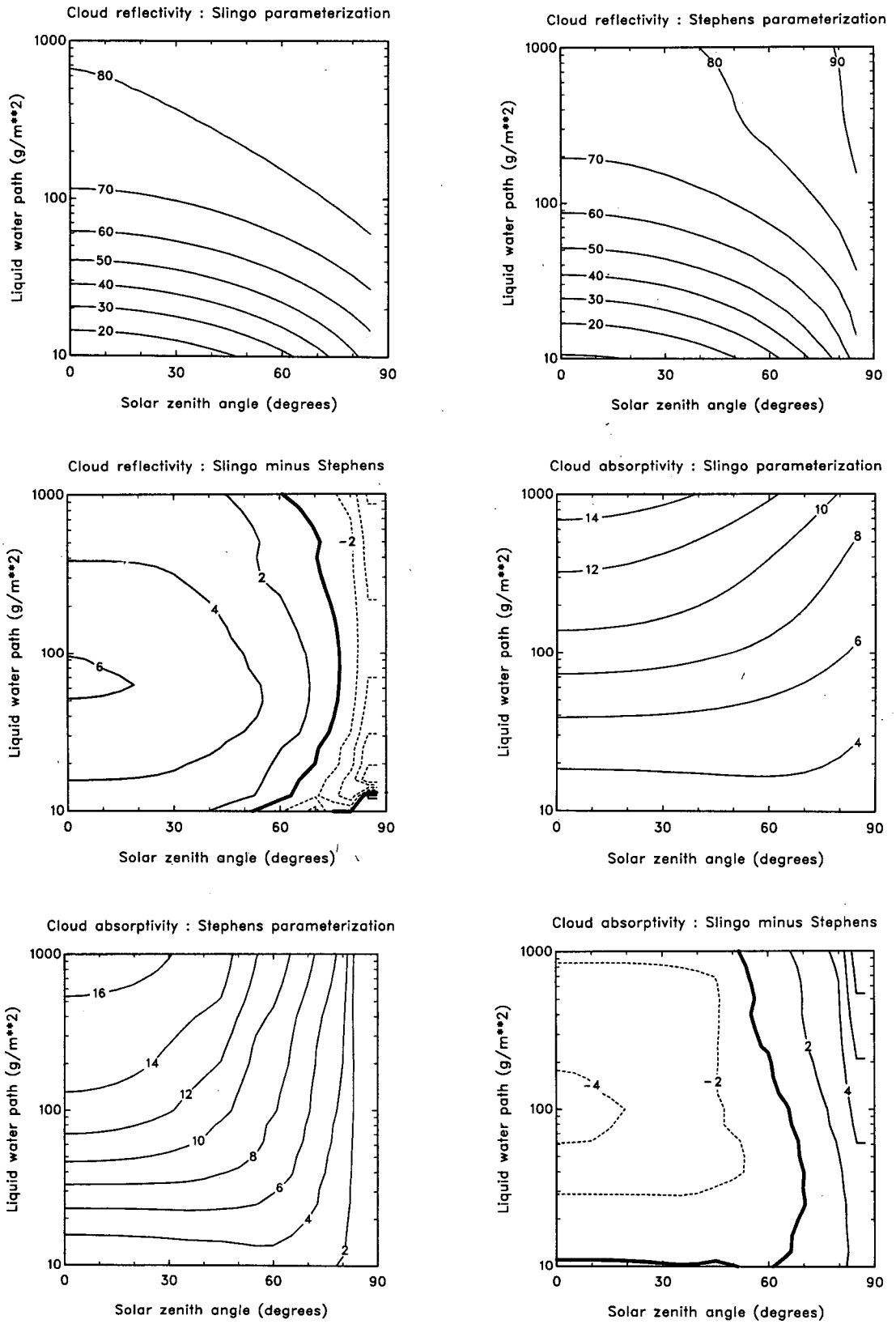

FIG. 1. Reflectivity and absorptivity of water clouds (percent) as functions of the cloud liquid water path and solar zenith angle. Results are shown for the present parameterization, that described by Stephens et al. (1984) and for the difference between the two.

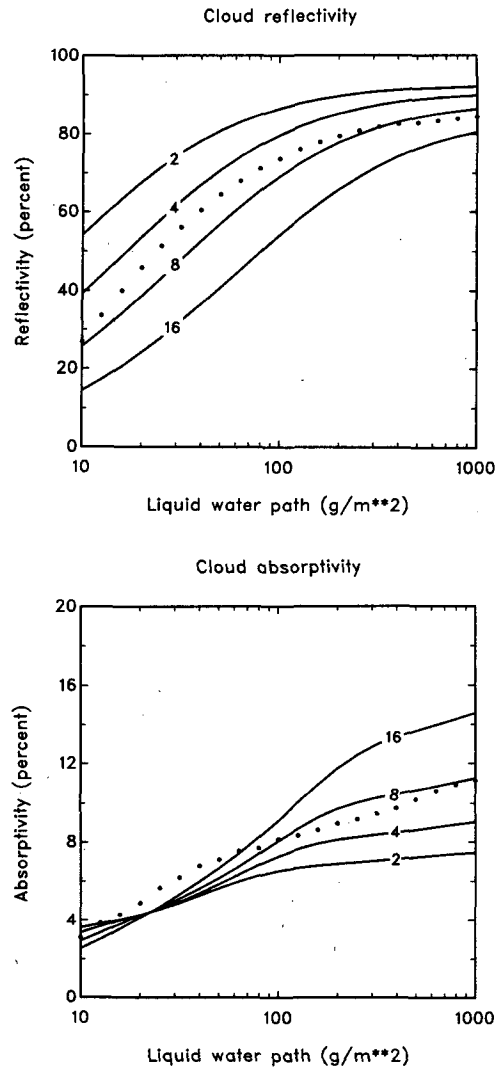

FIG. 2. Reflectivity and absorptivity of water clouds (percent) at a zenith angle of 60° as a function of the cloud liquid water path. Results from the Stephens et al. (1984) parameterization are shown as the dots. Results from the present work for various values of the equivalent radius (μm) are shown as the solid lines.

the drop size distribution. The value of this feature is demonstrated in Fig. 2, which shows the cloud radiative properties as functions of the liquid water path for four values of the equivalent radius. The dependence on r_e is particularly strong for the reflectivity. Results from Stephens' parameterization are shown as the dotted lines. The dependence on LWP is similar to that from the present work, the tendency for the dotted line to cross the 8 μm solid line being a reflection of the slow changes in the effective value of r_e implied by Stephens' liquid water path to optical depth relationship.

5. Discussion

A new parameterization for the shortwave radiative properties of water clouds which is suitable for inclusion in GCMs has been presented. Tests against a more detailed radiation code, the parameterization developed by Stephens et al. (1984) and against aircraft observations show that the parameterization gives good results, even with only four spectral bands. This spectral resolution probably also represents the minimum in order to reproduce the substantial wavelength dependence of surface albedos. The spectral divisions of the 4-band scheme denoted 10, 6, 5 and 3 (at about 0.69, 1.19 and 2.38 μm) were in part chosen because of the large changes in the albedo of vegetated surfaces at about 0.7 μm and of snow surfaces at about 1.2 μm (e.g., Fig. 1 of Davis et al. 1984). With this number of bands only four sets of coefficients need to be stored, the values of which for this version are given at the bottom of Table 1.

The most important new feature of the present scheme is the separation of the dependence of the cloud radiative properties on the liquid water path and equivalent radius of the drop size distribution. This makes the parameterization suitable for investigations of the effect on climate of independent changes in these two parameters. Neither of the parameterizations developed by Stephens et al. (1984) and by Liou and Wittman (1979) include such a feature, which limits their applicability to such work. In addition, the present scheme includes no tunable parameters which might limit its generality. The only important approximations used are the relationships found by Slingo and Schrecker (1982) between the single scattering properties of cloud drops and the liquid water path and equivalent radius. However, since these were based on only eight drop spectra, a wider range of observed and/or synthetic spectra are needed to provide more reliable values for the coefficients in Table 1.

As noted earlier, the neglect of water vapor absorption within the cloud can lead to an underestimate of the cloud absorption. However, the effect of water vapor may be included easily when the scheme is implemented in a GCM. The factor by which the water vapor path is enhanced by multiple scattering within cloud can be related to the cloud optical depth. The gaseous absorption may then be calculated using whatever technique is employed in the GCM and incorporated by multiplying the gaseous and droplet transmissivities in the appropriate spectral band. This approach is being followed in the NCAR Community Climate Model.

Acknowledgments. Some of this work was carried out at the U.K. Meteorological Office. The figures were produced by the graphics package GF, developed by Chuck D'Ambra and Starley Thompson at NCAR.

REFERENCES

Charlson, R. J., J. E. Lovelock, M. O. Andreae and S. G. Warren, 1987: Oceanic phytoplankton, atmospheric sulphur, cloud albedo and climate. *Nature*, **326**, 655–661.

Coakley, J. A., R. L. Bernstein and P. A. Durkee, 1987: Effect of ship–stack effluents on cloud reflectivity. *Science,* **237,** 1020–1022.

Davies, R., W. L. Ridgway and K.-E. Kim, 1984: Spectral absorption of solar radiation in cloudy atmospheres: a 20 cm^{-1} model. *J. Atmos. Sci.,* **41,** 2126–2137.

Davis, P. A., E. R. Major and H. Jacobowitz, 1984: An assessment of NIMBUS 7 ERB shortwave scanner data by correlative analysis with narrowband CZCS data. *J. Geophys. Res.,* **89,** 5077–5088.

Foot, J. S., 1988: Some observations of the optical properties of clouds. I: Stratocumulus. *Quart. J. Roy. Meteor. Soc.,* **114,** 129–144.

Herman, G. F., and J. A. Curry, 1984: Observational and theoretical studies of solar radiation in arctic stratus clouds. *J. Climate Appl. Meteor.,* **23,** 5–24.

Hignett, P., 1987: A study of the short-wave radiative properties of marine stratus: Aircraft measurements and model comparisons. *Quart. J. Roy. Meteor. Soc.,* **113,** 1011–1024.

Kratz, D. P., and R. P. Cess, 1985: Solar absorption by atmospheric water vapor: a comparison of radiation models. *Tellus,* **37B,** 53–63.

Lacis, A. A., and J. E. Hansen, 1974: A parameterization for the absorption of solar radiation in the earth's atmosphere. *J. Atmos. Sci.,* **31,** 118 –133.

Liou, K.-N., and G. D. Wittman, 1979: Parameterization of the radiative properties of clouds. *J. Atmos. Sci.,* **36,** 1261–1273.

Nicholls, S., 1984: The dynamics of stratocumulus: Aircraft observations and comparisons with a mixed layer model. *Quart. J. Roy. Meteor. Soc.,* **110,** 783–820.

——, and J. Leighton, 1986: An observational study of the structure of stratiform cloud sheets. Part I: Structure. *Quart. J. Roy. Meteor. Soc.,* **112,** 431–460.

Paltridge, G. W., 1980: Cloud–radiation feedback to climate. *Quart. J. Roy. Meteor. Soc.,* **106,** 895–899.

Roeckner, E., U. Schlese, J. Biercamp and P. Loewe, 1987: Cloud optical depth feedbacks and climate modelling. *Nature,* **329,** 138–140.

Schlesinger, M. E., and J. F. B. Mitchell, 1987: Climate model simulations of the equilibrium climatic response to increased carbon dioxide. *Rev. Geophys.,* **25,** 760–798.

Slingo, A., and H. M. Schrecker, 1982: On the shortwave radiative properties of stratiform water clouds. *Quart. J. Roy. Meteor. Soc.,* **108,** 407–426.

——, and D. W. Pearson, 1987: A comparison of the impact of an envelope orography and of a parameterization of orographic gravity-wave drag on model simulations. *Quart. J. Roy. Meteor. Soc.,* **113,** 847–870.

——, S. Nicholls and J. Schmetz, 1982: Aircraft observations of marine stratocumulus during JASIN. *Quart. J. Roy. Meteor. Soc.,* **108,** 833–856.

Somerville, R. C. J., and L. A. Remer, 1984: Cloud optical thickness feedbacks in the CO_2 climate problem. *J. Geophys. Res.,* **89,** 9668–9672.

Stephens, G. L., 1978: Radiation profiles in extended water clouds. II: Parameterization schemes. *J. Atmos. Sci.,* **35,** 2123–2132.

——, 1984: The parameterization of radiation for numerical weather prediction and climate models. *Mon. Wea. Rev.,* **112,** 826–867.

——, S. Ackerman and E. A. Smith, 1984: A shortwave parameterization revised to improve cloud absorption. *J. Atmos. Sci.,* **41,** 687–690.

Thekaekara, M. P., and A. J. Drummond, 1971: Standard values for the solar constant and its spectral components. *Nature Phys. Sci.,* **229,** 6–9.

Twomey, S. A., M. Piepgrass and T. L. Wolfe, 1984: An assessment of the impact of pollution on global cloud albedo. *Tellus,* **36B,** 356–366.

Wetherald, R. T., and S. Manabe, 1988: Cloud feedback processes in a general circulation model. *J. Atmos. Sci.,* **45,** 1397–1415.

Wiscombe, W. J., 1977: The Delta–Eddington approximation for a vertically inhomogeneous atmosphere. NCAR Tech. Note NCAR/TN-121+STR, 66 pp.

Zdunkowski, W. G., R. M. Welch and G. Korb, 1980: An investigation of the structure of typical two-stream-methods for the calculation of solar fluxes and heating rates in clouds. *Contrib. Atmos. Phys.,* **53,** 147–166.

——, W.-G. Panhans, R. M. Welch and G. J. Korb, 1982: A radiation scheme for circulation and climate models. *Contrib. Atmos. Phys.,* **55,** 215–238.